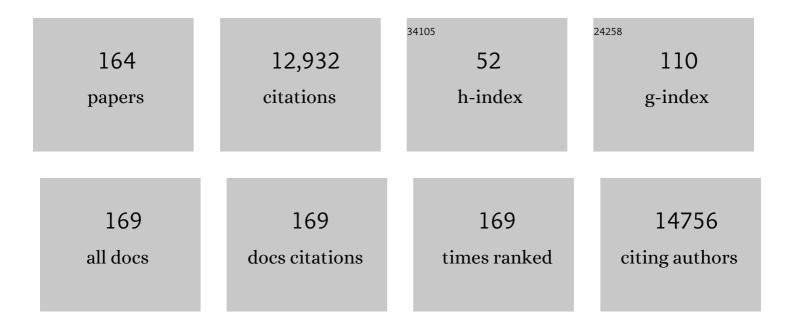
List of Publications by Year in descending order

Source: https://exaly.com/author-pdf/3201676/publications.pdf Version: 2024-02-01



#	Article	IF	CITATIONS
1	Phase coexistence in fluidization. AICHE Journal, 2022, 68, .	3.6	4
2	Rational Design of Zinc/Zeolite Catalyst: Selective Formation of <i>p</i> â€Xylene from Methanol to Aromatics Reaction. Angewandte Chemie - International Edition, 2022, 61, .	13.8	22
3	Innentitelbild: Rational Design of Zinc/Zeolite Catalyst: Selective Formation of <i>p</i> â€Xylene from Methanol to Aromatics Reaction (Angew. Chem. 10/2022). Angewandte Chemie, 2022, 134, .	2.0	0
4	Advances in Precise Structure Control and Assembly toward the Carbon Nanotube Industry (Adv.) Tj ETQq0 0	0 rgBT /Qvei 14.9	rlock 10 Tf 50
5	Advances in Precise Structure Control and Assembly toward the Carbon Nanotube Industry. Advanced Functional Materials, 2022, 32, .	14.9	12
6	In situ imaging of the sorption-induced subcell topological flexibility of a rigid zeolite framework. Science, 2022, 376, 491-496.	12.6	62
7	Modulating inherent lewis acidity at the intergrowth interface of mortise-tenon zeolite catalyst. Nature Communications, 2022, 13, .	12.8	9
8	Monochromatic Carbon Nanotube Tangles Grown by Microfluidic Switching between Chaos and Fractals. ACS Nano, 2021, 15, 5129-5137.	14.6	5
9	Resolving atomic SAPO-34/18 intergrowth architectures for methanol conversion by identifying light atoms and bonds. Nature Communications, 2021, 12, 2212.	12.8	33
10	A single-molecule van der Waals compass. Nature, 2021, 592, 541-544.	27.8	75
11	High-Performance Graphene/Carbon Nanotube-Based Adsorbents for Treating Diluted o-Cresol in Water in a Pilot-Plant Scale Demo. ACS Applied Materials & Interfaces, 2021, 13, 43266-43272.	8.0	1
12	Mechanical Behavior of Single and Bundled Defect-Free Carbon Nanotubes. Accounts of Materials Research, 2021, 2, 998-1009.	11.7	14
13	Ultrafast Nonvolatile Ionic Liquids-Based Supercapacitors with Al Foam-Enhanced Carbon Electrode. ACS Applied Materials & Interfaces, 2021, 13, 53904-53914.	8.0	4
14	Material Compatibility of Hexamethyldisiloxane as Organic Rankine Cycle Working Fluids at High Temperatures. Journal of Thermal Science, 2020, 29, 25-31.	1.9	3
15	Process simulation of the syngas-to-aromatics processes: Technical economics aspects. Chemical Engineering Science, 2020, 212, 115328.	3.8	15
16	The Application of Carbon Nanotube/Grapheneâ€Based Nanomaterials in Wastewater Treatment. Small, 2020, 16, e1902301.	10.0	109
17	High energy and high power density supercapacitor with 3D Al foam-based thick graphene electrode: Fabrication and simulation. Energy Storage Materials, 2020, 33, 18-25.	18.0	48
18	Decentralized methanol feed in a two-stage fluidized bed for process intensification of methanol to aromatics. Chemical Engineering and Processing: Process Intensification, 2020, 154, 108049.	3.6	9

#	Article	IF	CITATIONS
19	Temperature-dependent secondary conversion of primary products from methanol aromatization in a two-stage fluidized bed. Fuel, 2020, 267, 117204.	6.4	13
20	A nitrogen-doped mesopore-dominated carbon electrode allied with anti-freezing EMIBF <sub>4</sub> –CBL electrolyte for superior low-temperature supercapacitors. Journal of Materials Chemistry A, 2020, 8, 10386-10394.	10.3	21
21	Catalytic methane technology for carbon nanotubes and graphene. Reaction Chemistry and Engineering, 2020, 5, 991-1004.	3.7	16
22	Insight into the Effects of Water on the Ethene to Aromatics Reaction with HZSM-5. ACS Catalysis, 2020, 10, 5288-5298.	11.2	39
23	Highly electroconductive mesoporous activated carbon fibers and their performance in the ionic liquid-based electrical double-layer capacitors. Carbon, 2019, 154, 1-6.	10.3	39
24	Enhanced production of aromatics from propane with a temperature-shifting two-stage fluidized bed reactor. RSC Advances, 2019, 9, 26532-26536.	3.6	7
25	Review of the Working Fluid Thermal Stability for Organic Rankine Cycles. Journal of Thermal Science, 2019, 28, 597-607.	1.9	31
26	Highly selective conversion of methanol to propylene: design of an MFI zeolite with selective blockage of (010) surfaces. Nanoscale, 2019, 11, 8096-8101.	5.6	14
27	3D Hierarchical Porous Graphene-Based Energy Materials: Synthesis, Functionalization, and Application in Energy Storage and Conversion. Electrochemical Energy Reviews, 2019, 2, 332-371.	25.5	82
28	A multi-stage fluidized bed strategy for the enhanced conversion of methanol into aromatics. Chemical Engineering Science, 2019, 204, 1-8.	3.8	26
29	High-yield production of aromatics from methanol using a temperature-shifting multi-stage fluidized bed reactor technology. Chemical Engineering Journal, 2019, 371, 639-646.	12.7	31
30	Thermal stability of hexamethyldisiloxane (MM) as a working fluid for organic Rankine cycle. International Journal of Energy Research, 2019, 43, 896-904.	4.5	24
31	Modulation of b-axis thickness within MFI zeolite: Correlation with variation of product diffusion and coke distribution in the methanol-to-hydrocarbons conversion. Applied Catalysis B: Environmental, 2019, 243, 721-733.	20.2	71
32	Heterogeneous catalysis in multiâ€stage fluidized bed reactors: From fundamental study to industrial application. Canadian Journal of Chemical Engineering, 2019, 97, 636-644.	1.7	10
33	Carbon nanotube- and graphene-based nanomaterials and applications in high-voltage supercapacitor: A review. Carbon, 2019, 141, 467-480.	10.3	610
34	Perspective to the Potential Use of Graphene in Liâ€ion Battery and Supercapacitor. Chemical Record, 2019, 19, 1256-1262.	5.8	17
35	Resilient, mesoporous carbon nanotube-based strips as adsorbents of dilute organics in water. Carbon, 2018, 132, 329-334.	10.3	21
36	Mesoporous tubular graphene electrode for high performance supercapacitor. Chinese Chemical Letters, 2018, 29, 599-602.	9.0	21

#	Article	IF	CITATIONS
37	Crystal-plane effects of MFI zeolite in catalytic conversion of methanol to hydrocarbons. Journal of Catalysis, 2018, 360, 89-96.	6.2	58
38	EMIMBF <sub>4</sub> –GBL binary electrolyte working at â^70 °C and 3.7 V for a high performance graphene-based capacitor. Journal of Materials Chemistry A, 2018, 6, 3593-3601.	10.3	46
39	Flexible metal-templated fabrication of mesoporous onion-like carbon and Fe <sub>2</sub> O <sub>3</sub> @N-doped carbon foam for electrochemical energy storage. Journal of Materials Chemistry A, 2018, 6, 13012-13020.	10.3	44
40	Carbon nanotube-alumina strips as robust, rapid, reversible adsorbents of organics. RSC Advances, 2018, 8, 10715-10718.	3.6	5
41	Reaction and deactivation of propylene over SAPO-34 at low temperature. Catalysis Today, 2018, 301, 244-247.	4.4	8
42	Experimental study of non-uniform bubble growth in deep fluidized beds. Chemical Engineering Science, 2018, 176, 515-523.	3.8	23
43	Thermal stability of some hydrofluorocarbons as supercritical ORCs working fluids. Applied Thermal Engineering, 2018, 128, 1095-1101.	6.0	59
44	Regulation of Ni–CNT Interaction on Mn-Promoted Nickel Nanocatalysts Supported on Oxygenated CNTs for CO <sub>2</sub> Selective Hydrogenation. ACS Applied Materials & Interfaces, 2018, 10, 41224-41236.	8.0	45
45	Cross oupled Macroâ€Mesoporous Carbon Network toward Record High Energyâ€Power Density Supercapacitor at 4 V. Advanced Functional Materials, 2018, 28, 1806153.	14.9	145
46	Influence of alkane working fluid decomposition on supercritical organic Rankine cycle systems. Energy, 2018, 153, 422-430.	8.8	19
47	Analyzing transfer properties of zeolites using small-world networks. Nanoscale, 2018, 10, 16431-16433.	5.6	9
48	Highly selective synthesis of large aromatic molecules with nano-zeolite: beyond the shape selectivity effect. RSC Advances, 2017, 7, 14309-14313.	3.6	15
49	Graphene-carbon nanotube hybrids as robust, rapid, reversible adsorbents for organics. Carbon, 2017, 116, 409-414.	10.3	13
50	Screening of working fluids and metal materials for high temperature organic Rankine cycles by compatibility. Journal of Renewable and Sustainable Energy, 2017, 9, .	2.0	17
51	High yield production of C <sub>2</sub> –C <sub>3</sub> olefins and para-xylene from methanol using a SiO <sub>2</sub> -coated FeO <sub>x</sub> /ZSM-5 catalyst. RSC Advances, 2017, 7, 28940-28944.	3.6	10
52	Seed-induced and additive-free synthesis of oriented nanorod-assembled meso/macroporous zeolites: toward efficient and cost-effective catalysts for the MTA reaction. Catalysis Science and Technology, 2017, 7, 5143-5153.	4.1	26
53	Instability of uniform fluidization. Chemical Engineering Science, 2017, 173, 187-195.	3.8	12
54	The analysis of hot spots in large scale fluidized bed reactors. RSC Advances, 2017, 7, 20186-20191.	3.6	5

#	Article	IF	CITATIONS
55	Design of parallel cyclones based on stability analysis. AICHE Journal, 2016, 62, 4251-4258.	3.6	14
56	The influence of straight pore blockage on the selectivity of methanol to aromatics in nanosized Zn/ZSM-5: an atomic Cs-corrected STEM analysis study. RSC Advances, 2016, 6, 74797-74801.	3.6	48
57	Molded MFI nanocrystals as a highly active catalyst in a methanol-to-aromatics process. RSC Advances, 2016, 6, 81198-81202.	3.6	21
58	Screening of hydrocarbons as supercritical ORCs working fluids by thermal stability. Energy Conversion and Management, 2016, 126, 632-637.	9.2	82
59	Fabrication and catalytic properties of three-dimensional ordered zeolite arrays with interconnected micro-meso-macroporous structure. Journal of Materials Chemistry A, 2016, 4, 10834-10841.	10.3	22
60	Interwall Friction and Sliding Behavior of Centimeters Long Double-Walled Carbon Nanotubes. Nano Letters, 2016, 16, 1367-1374.	9.1	36
61	Bayberry-like ZnO/MFI zeolite as high performance methanol-to-aromatics catalyst. Chemical Communications, 2016, 52, 2011-2014.	4.1	77
62	Equilibrium analysis of methylbenzene intermediates for a methanol-to-olefins process. Catalysis Science and Technology, 2016, 6, 1297-1301.	4.1	19
63	Chemical kinetics method for evaluating the thermal stability of Organic Rankine Cycle working fluids. Applied Thermal Engineering, 2016, 100, 708-713.	6.0	49
64	Crystal-plane effect of nanoscale CeO <sub>2</sub> on the catalytic performance of Ni/CeO <sub>2</sub> catalysts for methane dry reforming. Catalysis Science and Technology, 2016, 6, 3594-3605.	4.1	170
65	Conversion of methanol with C5–C6 hydrocarbons into aromatics in a two-stage fluidized bed reactor. Catalysis Today, 2016, 264, 63-69.	4.4	32
66	Enhancing 5 V capacitor performance by adding single walled carbon nanotubes into an ionic liquid electrolyte. Journal of Materials Chemistry A, 2015, 3, 15858-15862.	10.3	11
67	Ion-Responsive Channels of Zwitterion-Carbon Nanotube Membrane for Rapid Water Permeation and Ultrahigh Mono-/Multivalent Ion Selectivity. ACS Nano, 2015, 9, 7488-7496.	14.6	107
68	Increasing <i>para</i> -Xylene Selectivity in Making Aromatics from Methanol with a Surface-Modified Zn/P/ZSM-5 Catalyst. ACS Catalysis, 2015, 5, 2982-2988.	11.2	263
69	Full capacitance potential of SWCNT electrode in ionic liquids at 4 V. Journal of Materials Chemistry A, 2014, 2, 19897-19902.	10.3	17
70	Oneâ€pot Synthesis of Ordered Mesoporous NiCeAl Oxide Catalysts and a Study of Their Performance in Methane Dry Reforming. ChemCatChem, 2014, 6, 1470-1480.	3.7	38
71	Centrifugation-free and high yield synthesis of nanosized H-ZSM-5 and its structure-guided aromatization of methanol to 1,2,4-trimethylbenzene. Journal of Materials Chemistry A, 2014, 2, 19797-19808.	10.3	76
72	Conversion of methanol to aromatics in fluidized bed reactor. Catalysis Today, 2014, 233, 8-13.	4.4	84

#	Article	IF	CITATIONS
73	Atmospheric pressure synthesis of nanosized ZSM-5 with enhanced catalytic performance for methanol to aromatics reaction. Catalysis Science and Technology, 2014, 4, 3840-3844.	4.1	72
74	Highly Electroconductive Mesoporous Graphene Nanofibers and Their Capacitance Performance at 4 V. Journal of the American Chemical Society, 2014, 136, 2256-2259.	13.7	192
75	Correction to Growth of Half-Meter Long Carbon Nanotubes Based on Schulz–Flory Distribution. ACS Nano, 2014, 8, 3097-3097.	14.6	2
76	Highly selective synthesis of single-walled carbon nanotubes from methane in a coupled Downer-turbulent fluidized-bed reactor. Journal of Energy Chemistry, 2013, 22, 567-572.	12.9	11
77	High-yield Synthesis of Nanohybrid Shish-kebab Polyethylene-carbon Nanotube Structure. Chinese Journal of Chemical Engineering, 2013, 21, 37-43.	3.5	3
78	Facile manipulation of individual carbon nanotubes assisted by inorganic nanoparticles. Nanoscale, 2013, 5, 6584.	5.6	12
79	Preparation and characterization of a plasma treated NiMgSBA-15 catalyst for methane reforming with CO2 to produce syngas. Catalysis Science and Technology, 2013, 3, 2278.	4.1	94
80	Highly deformation-tolerant carbon nanotube sponges as supercapacitor electrodes. Nanoscale, 2013, 5, 8472.	5.6	101
81	Ionic liquid coated single-walled carbon nanotube buckypaper as supercapacitor electrode. Particuology, 2013, 11, 409-414.	3.6	28
82	Raising the performance of a 4 V supercapacitor based on an EMIBF4–single walled carbon nanotube nanofluid electrolyte. Chemical Communications, 2013, 49, 10727.	4.1	41
83	Superlubricity in centimetres-long double-walled carbon nanotubes under ambient conditions. Nature Nanotechnology, 2013, 8, 912-916.	31.5	305
84	MgO-catalyzed growth of N-doped wrinkled carbon nanotubes. Carbon, 2013, 56, 38-44.	10.3	48
85	Synthesis of graphene from asphaltene molecules adsorbed on vermiculite layers. Carbon, 2013, 62, 213-221.	10.3	63
86	Formation mechanism of carbon encapsulated Fe nanoparticles in the growth of single-/double-walled carbon nanotubes. Chemical Engineering Journal, 2013, 223, 617-622.	12.7	11
87	Chemical vapor deposition derived flexible graphene paper and its application as high performance anodes for lithium rechargeable batteries. Journal of Materials Chemistry A, 2013, 1, 408-414.	10.3	78
88	Direct synthesis of c-axis oriented ZSM-5 nanoneedles from acid-treated kaolin clay. Journal of Materials Chemistry A, 2013, 1, 3272.	10.3	53
89	The reason for the low density of horizontally aligned ultralong carbon nanotube arrays. Carbon, 2013, 52, 232-238.	10.3	27
90	High strength composites using interlocking carbon nanotubes in a polyimide matrix. Carbon, 2013, 60, 102-108.	10.3	14

#	Article	IF	CITATIONS
91	Synthesis, characterization and catalytic performance of MgO-coated Ni/SBA-15 catalysts for methane dry reforming to syngas and hydrogen. International Journal of Hydrogen Energy, 2013, 38, 9718-9731.	7.1	131
92	Ferromagnetism in nanomesh graphene. Carbon, 2013, 51, 390-396.	10.3	52
93	Multi-walled carbon nanotube-based carbon/carbon composites with three-dimensional network structures. Nanoscale, 2013, 5, 6181.	5.6	27
94	Facile Route for Synthesizing Ordered Mesoporous Ni–Ce–Al Oxide Materials and Their Catalytic Performance for Methane Dry Reforming to Hydrogen and Syngas. ACS Catalysis, 2013, 3, 1638-1651.	11.2	362
95	Growth of Half-Meter Long Carbon Nanotubes Based on Schulz–Flory Distribution. ACS Nano, 2013, 7, 6156-6161.	14.6	308
96	Carbon nanotube production and application in energy storage. Asia-Pacific Journal of Chemical Engineering, 2013, 8, 234-245.	1.5	23
97	Fabrication of <i>c-</i> Axis Oriented ZSM-5 Hollow Fibers Based on an in Situ Solid–Solid Transformation Mechanism. Journal of the American Chemical Society, 2013, 135, 15322-15325.	13.7	110
98	碳纳米管的å®é‡å^¶å <b>¤</b> åŠäº§ä¸šåŒ–. Scientia Sinica Chimica, 2013, 43, 641-666.	0.4	5
99	Carbon nanotubes for supercapacitors: Consideration of cost and chemical vapor deposition techniques. Journal of Natural Gas Chemistry, 2012, 21, 233-240.	1.8	38
100	Hierarchical carbon nanotube membrane with high packing density and tunable porous structure for high voltage supercapacitors. Carbon, 2012, 50, 5167-5175.	10.3	87
101	Nanobelt–carbon nanotube cross-junction solar cells. Energy and Environmental Science, 2012, 5, 6119.	30.8	11
102	Integrating carbon nanotube into activated carbon matrix for improving the performance of supercapacitor. Materials Science and Engineering B: Solid-State Materials for Advanced Technology, 2012, 177, 1138-1143.	3.5	27
103	Dramatic enhancements in toughness of polyimide nanocomposite via long-CNT-induced long-range creep. Journal of Materials Chemistry, 2012, 22, 7050.	6.7	63
104	High capacity gas storage in corrugated porous graphene with a specific surface area-lossless tightly stacking manner. Chemical Communications, 2012, 48, 6815.	4.1	79
105	One-step synthesis of a graphene-carbon nanotube hybrid decorated by magnetic nanoparticles. Carbon, 2012, 50, 2764-2771.	10.3	64
106	Gram-scale synthesis of nanomesh graphene with high surface area and its application in supercapacitor electrodes. Chemical Communications, 2011, 47, 5976.	4.1	339
107	Architectural and mechanical performances of carbon nanotube agglomerates characterized by compaction response. Powder Technology, 2011, 211, 226-231.	4.2	9
108	Superstrong Ultralong Carbon Nanotubes for Mechanical Energy Storage. Advanced Materials, 2011, 23, 3387-3391.	21.0	170

WEIZHONG QIAN

#	Article	IF	CITATIONS
109	Enhanced Catalytic Activity of Subâ€nanometer Titania Clusters Confined inside Doubleâ€Wall Carbon Nanotubes. ChemSusChem, 2011, 4, 975-980.	6.8	57
110	Synthesis of high quality single-walled carbon nanotubes on natural sepiolite and their use for phenol absorption. Carbon, 2011, 49, 1568-1580.	10.3	36
111	Enhanced actuation in functionalized carbon nanotube–Nafion composites. Sensors and Actuators B: Chemical, 2011, 156, 187-193.	7.8	55
112	100 mm Long, Semiconducting Tripleâ€Walled Carbon Nanotubes. Advanced Materials, 2010, 22, 1867-187	121.0	91
113	A Threeâ€Dimensional Carbon Nanotube/Graphene Sandwich and Its Application as Electrode in Supercapacitors. Advanced Materials, 2010, 22, 3723-3728.	21.0	1,182
114	Preparation of graphene nanosheet/carbon nanotube/polyaniline composite as electrode material for supercapacitors. Journal of Power Sources, 2010, 195, 3041-3045.	7.8	540
115	Super resilience of a compacted mixture of natural graphite and agglomerated carbon nanotubes under cyclic compression. Carbon, 2010, 48, 309-312.	10.3	6
116	Preparation of a graphene nanosheet/polyaniline composite with high specific capacitance. Carbon, 2010, 48, 487-493.	10.3	999
117	Electrochemical properties of graphene nanosheet/carbon black composites as electrodes for supercapacitors. Carbon, 2010, 48, 1731-1737.	10.3	534
118	Fast and reversible surface redox reaction of graphene–MnO2 composites as supercapacitor electrodes. Carbon, 2010, 48, 3825-3833.	10.3	1,272
119	Oil sorption and recovery by using vertically aligned carbon nanotubes. Carbon, 2010, 48, 4197-4200.	10.3	44
120	Nano-size MZnAl (M=Cu, Co, Ni) metal oxides obtained by combining hydrothermal synthesis with urea homogeneous precipitation procedures. Applied Clay Science, 2010, 48, 203-207.	5.2	37
121	Granulated Carbon Nanotubes as the Catalyst Support for Pt for the Hydrogenation of Nitrobenzene. Australian Journal of Chemistry, 2010, 63, 131.	0.9	16
122	Growing 20 cm Long DWNTs/TWNTs at a Rapid Growth Rate of 80â^'90 μm/s. Chemistry of Materials, 2010, 22, 1294-1296.	6.7	88
123	Large area growth of aligned CNT arrays on spheres: Cost performance and product control. Materials Letters, 2009, 63, 84-87.	2.6	23
124	Energyâ€Absorbing Hybrid Composites Based on Alternate Carbonâ€Nanotube and Inorganic Layers. Advanced Materials, 2009, 21, 2876-2880.	21.0	118
125	Synthesis of Highâ€Quality, Doubleâ€Walled Carbon Nanotubes in a Fluidized Bed Reactor. Chemical Engineering and Technology, 2009, 32, 73-79.	1.5	41
126	Preparation of exfoliated graphite containing manganese oxides with high electrochemical capacitance by microwave irradiation. Carbon, 2009, 47, 3371-3374.	10.3	25

WEIZHONG QIAN

#	Article	IF	CITATIONS
127	Synthesis of well-dispersed ZnO nanomaterials by directly calcining zinc stearate. Journal of Alloys and Compounds, 2009, 472, 343-346.	5.5	8
128	Gas-Phase Catalytic Hydrochlorination of Acetylene in a Two-Stage Fluidized-Bed Reactor. Industrial & Engineering Chemistry Research, 2009, 48, 128-133.	3.7	61
129	Very High-Quality Single-Walled Carbon Nanotubes Grown Using a Structured and Tunable Porous Fe/MgO Catalyst. Journal of Physical Chemistry C, 2009, 113, 20178-20183.	3.1	21
130	High Selectivity Production of Propylene from n-Butene: Thermodynamic and Experimental Study Using a Shape Selective Zeolite Catalyst. Catalysis Letters, 2008, 125, 380-385.	2.6	21
131	Synthesis of Single-Walled Carbon Nanotubes with Narrow Diameter Distribution by Calcination of a Mo-Modified Fe/MgO Catalyst. Chinese Journal of Catalysis, 2008, 29, 617-623.	14.0	16
132	Selective Synthesis of Single/Double/Multi-walled Carbon Nanotubes on MgO-Supported Fe Catalyst. Chinese Journal of Catalysis, 2008, 29, 1138-1144.	14.0	24
133	Liquefied petroleum gas containing sulfur as the carbon source for carbon nanotube forests. Carbon, 2008, 46, 291-296.	10.3	42
134	In situ growth of carbon nanotubes on inorganic fibers with different surface properties. Materials Chemistry and Physics, 2008, 107, 317-321.	4.0	30
135	Growth Deceleration of Vertically Aligned Carbon Nanotube Arrays:  Catalyst Deactivation or Feedstock Diffusion Controlled?. Journal of Physical Chemistry C, 2008, 112, 4892-4896.	3.1	102
136	Hierarchical Agglomerates of Carbon Nanotubes as High-Pressure Cushions. Nano Letters, 2008, 8, 1323-1327.	9.1	50
137	Synthesis of thin-walled carbon nanotubes from methane by changing the Ni/Mo ratio in a Ni/Mo/MgO catalyst. New Carbon Materials, 2008, 23, 319-325.	6.1	20
138	Enhanced Activation and Decomposition of CH <sub>4</sub> by the Addition of C <sub>2</sub> H <sub>4</sub> or C <sub>2</sub> H <sub>2</sub> for Hydrogen and Carbon Nanotube Production. Journal of Physical Chemistry C, 2008, 112, 7588-7593.	3.1	33
139	Large scale synthesis of vertical aligned CNT array on irregular quartz particles. Materials Research Society Symposia Proceedings, 2008, 1081, 1.	0.1	0
140	SYNTHESIS OF SINGLE-WALLED CARBON NANOTUBES FROM LIQUEFIED PETROLEUM GAS. Nano, 2008, 03, 95-100.	1.0	11
141	Synthesis of Vertically Aligned CNTs with Hollow Channel on Al[sub 2]O[sub 3]–Al Substrate Electroplated with Fe Nanoparticles. Journal of the Electrochemical Society, 2008, 155, K180.	2.9	10
142	FEW WALLED CARBON NANOTUBE PRODUCTION IN LARGE-SCALE BY NANO-AGGLOMERATE FLUIDIZED-BED PROCESS. Nano, 2008, 03, 45-50.	1.0	18
143	Temperature effect on the substrate selectivity of carbon nanotube growth in floating chemical vapor deposition. Nanotechnology, 2007, 18, 415703.	2.6	29
144	Oxygen-assisted synthesis of SWNTs from methane decomposition. Nanotechnology, 2007, 18, 215610.	2.6	16

#	Article	IF	CITATIONS
145	CO2-Assisted SWNT Growth on Porous Catalysts. Chemistry of Materials, 2007, 19, 1226-1230.	6.7	71
146	Synchronous Growth of Vertically Aligned Carbon Nanotubes with Pristine Stress in the Heterogeneous Catalysis Process. Journal of Physical Chemistry C, 2007, 111, 14638-14643.	3.1	86
147	The effect of phase separation in Fe/Mg/Al/O catalysts on the synthesis of DWCNTs from methane. Carbon, 2007, 45, 1645-1650.	10.3	33
148	Large scale production of carbon nanotube arrays on the sphere surface from liquefied petroleum gas at low cost. Science Bulletin, 2007, 52, 2896-2902.	1.7	27
149	Synthesis of carbon nanotubes with totally hollow channels and/or with totally copper filled nanowires. Applied Physics A: Materials Science and Processing, 2006, 86, 265-269.	2.3	18
150	Synthesis of dispersed ZrO2 nano-laminae composed of ZrO2 nanocrystals. Materials Letters, 2006, 60, 3104-3108.	2.6	7
151	Gas-flow assisted bulk synthesis of V-type SnO2 nanowires. Journal of Crystal Growth, 2005, 285, 49-53.	1.5	12
152	Elastic deformation of multiwalled carbon nanotubes in electrospun MWCNTs–PEO and MWCNTs–PVA nanofibers. Polymer, 2005, 46, 12689-12695.	3.8	81
153	Gaseous catalytic hydrogenation of nitrobenzene to aniline in a two-stage fluidized bed reactor. Applied Catalysis A: General, 2005, 286, 30-35.	4.3	86
154	A novel low-temperature method to grow single-crystal ZnO nanorods. Journal of Crystal Growth, 2004, 271, 353-357.	1.5	43
155	Enhanced production of carbon nanotubes: combination of catalyst reduction and methane decomposition. Applied Catalysis A: General, 2004, 258, 121-124.	4.3	99
156	Carbon nanotubes containing iron and molybdenum particles as a catalyst for methane decomposition. Carbon, 2003, 41, 846-848.	10.3	32
157	Quantitative Raman characterization of the mixed samples of the single and multi-wall carbon nanotubes. Carbon, 2003, 41, 1851-1854.	10.3	92
158	Effect of adding nickel to iron–alumina catalysts on the morphology of as-grown carbon nanotubes. Carbon, 2003, 41, 2487-2493.	10.3	46
159	The evaluation of the gross defects of carbon nanotubes in a continuous CVD process. Carbon, 2003, 41, 2613-2617.	10.3	66
160	Carbon nanotubes with large cores produced by adding sodium carbonate to the catalyst. Carbon, 2003, 41, 2683-2686.	10.3	9
161	The formation mechanism of the coaxial carbon–metal nanowires in a chemical vapor deposition process. Solid State Communications, 2003, 126, 365-367.	1.9	13
162	What causes the carbon nanotubes collapse in a chemical vapor deposition process. Journal of Chemical Physics, 2003, 118, 878-882.	3.0	27

#	Article	IF	CITATIONS
163	Synthesis of carbon nanotubes from liquefied petroleum gas containing sulfur. Carbon, 2002, 40, 2968-2970.	10.3	84
164	Rational Design of Zinc/Zeolite Catalyst: Selective Formation of p â€Xylene from Methanol to Aromatics Reaction. Angewandte Chemie, 0, , .	2.0	1